15TH IEA HEAT PUMP CONFERENCE
MAY 26–29, 2026 | HOFBURG
VIENNA 2026
DECARBONISATION THROUGH INNOVATION

A Carnot-Based Pre-Screening Method to Support High-Temperature Heat Pump Integration in Industries

Mostafa Babaei [a*], Martin K. Patel [a]

[a] University of Geneva, Faculty of Science, Institute for Environmental Sciences (ISE) and Department F.-A. Forel (DEFSE), Boulevard Carl-Vogt 66, CH-1211 Genève 4, Switzerland

Abstract

Integrating high-temperature heat pumps (HTHPs) into manufacturing industries represents a promising pathway toward industrial decarbonization. However, traditional design approaches often rely on detailed modeling of working fluids and cycle configurations, making the process slow, complex, and difficult to scale. Moreover, design decisions such as sizing and temperature-level selection are frequently based on engineering intuition, which can lead to suboptimal solutions. This work introduces a flexible and automated pre-screening methodology based on Carnot heat pump principles, aimed at rapidly identifying optimal HTHP integration strategies. The method begins by generating Pinch-based profiles from process stream data to represent heating and cooling demands across different temperature levels. The resulting optimization problem is formulated as a Mixed-Integer Nonlinear Programming (MINLP) problem with strong nonconvexities and multiple local optima. To efficiently explore this complex design space, evolutionary algorithms such as the Genetic Algorithm (GA) are employed. The objective is to determine the number, size, temperature levels, and allocation of HTHPs that achieve the best trade-off between energy efficiency, expressed as the Coefficient of Performance (COP), and total cost. Solutions are evaluated using ideal Carnot performance to ensure thermodynamic feasibility and general applicability. This pre-screening step significantly narrows the design space for real-system optimization, enabling more computationally efficient exploration of detailed configurations. The model also allows rapid recalculations under varying energy or equipment prices, offering insights into cost-efficiency trade-offs. While increasing the number of heat pumps typically improves COP, it also raises capital cost; the proposed method identifies the optimal balance. A case study from the paper industry demonstrates that this approach can generate actionable results within seconds, providing a scalable foundation for subsequent optimization and real-world HTHP deployment.

© HPC2026.
Selection and/or peer-review under the responsibility of the organizers of the 15th IEA Heat Pump Conference 2026.

Keywords: High-temperature heat pump; Genetic Algorithm; Process integration; Optimization; Industrial decarbonization

1. Introduction

Industrial heat generation represents a large share of global final energy consumption and greenhouse-gas emissions [1]. In many energy-intensive sectors (e.g., pulp & paper, chemicals, food), a significant portion of process heat is required at medium-to-high temperatures (100–200 °C), making it a target for electrification via high-temperature heat pumps (HTHPs) [2]. Recent advancements in compressor technology, working fluids, and system design have extended feasible HTHP supply temperatures beyond 160 °C, enabling their use even for steam-generation applications [3].

Despite these technological improvements, integrating HTHPs into industrial plants is nontrivial [4]. The design involves multiple interdependent decisions: selecting temperature levels, sizing heat pumps, matching heat sources and sinks, and balancing capital and operating costs. Traditional methods frequently rely on

* Corresponding author. Tel.: +41 (0)22 379 06 39
E-mail address: Mostafa.babaei@unige.ch

detailed thermodynamic modeling of individual cycles and fluids [5]. These approaches yield high fidelity but are often slow, data-intensive, and difficult to generalize across processes. As a result, early-stage screening of integration options is rarely systematic and often relies on engineering heuristics, which risks overlooking promising design alternatives.

Literature background: Several efforts have explored heat pump integration in industrial contexts. Pinch-based methods for heat pump integration have been reviewed by Schlosser et al. [6], showing how vapor-compression heat pumps can be matched to process demands using Grand Composite Curve (GCC) analysis, and demonstrating typical Coefficient of Performance (COP) and temperature lifts in diverse industries (food, paper, chemical). Wallerand et al. [7], proposed a superstructure-based optimization approach for industrial heat pumps, selecting temperature levels, fluids, and capacities for integration in processes. More recently, Sharevska et al. [8], developed a component-to-system design methodology for multi-temperature HTHP integration in manufacturing energy systems. Analytical approaches using Lorenz- or break-even methods to estimate optimal heat pump sink temperatures have also been proposed [9]. These works contribute key insights, but typically either demand detailed cycle modeling or do not scale easily to large design spaces. To fill this gap, a fast, thermodynamically consistent pre-screening layer is needed. The goal is to rapidly filter out clearly unpromising configurations and guide detailed optimization toward the most plausible candidates.

To overcome these limitations, a multi-layered design framework is needed, one that couples the thermodynamic rigor of process integration with the flexibility of data-driven optimization. At its foundation, a fast-screening layer should identify feasible and promising temperature levels before invoking detailed cycle or fluid modeling. Such a layer can drastically reduce computational effort while maintaining thermodynamic relevance, forming the logical front-end of a larger superstructure-based optimization environment.

In this work, we propose a Carnot-based pre-screening methodology for industrial HTHP integration. Starting from Pinch-based profiles, the method estimates ideal heat pump performance across possible source–sink temperature pairs. The intuition is: if a configuration yields poor performance under ideal (Carnot) conditions, it will perform even worse in real-world cycles; conversely, configurations with favorable Carnot-level efficiency are prime candidates for more detailed study. This physically grounded approach helps narrow the design space at negligible computational cost.

Selecting the optimal number, capacity, and temperature levels of heat pumps entails both continuous (heat flows, temperatures) and discrete (number of units, activation choices) variables. This formulation leads to a Mixed-Integer Nonlinear Programming (MINLP) problem with nonconvexities and multiple local optima. Traditional deterministic solvers may stall or converge to local solutions. To address this, we employ evolutionary algorithms, particularly the Genetic Algorithm (GA), which are well-suited to explore multimodal, mixed-variable landscapes.

Compared with existing studies focused on cycle-level optimization or superstructure design, our method introduces a higher-level thermodynamically consistent filter that can operate on process data alone. The outputs of the pre-screening step can then feed into detailed superstructure optimization (with real-fluid thermodynamics and cost models). A case study from the Swiss paper industry demonstrates that actionable, high-quality screening results can be obtained with negligible computational effort, enabling scalable decision support for real-world HTHP deployment. The methodology and workflow are presented in Section 2.

2. Methodology

2.1. Overview of the workflow

The proposed methodology provides a fast and thermodynamically consistent way to identify promising configurations for HTHP integration before detailed real-fluid optimization. It consists of four main steps:

- Preparation of process data through Pinch analysis.
- Identification of feasible source (waste-heat) and sink (process-heating) temperature zones.
- Evaluation of potential evaporator–condenser placements using Carnot-based filtering method.
- Optimization of the number, size, and temperature levels of HTHPs to minimize Total Annual Cost (TAC).
- Evaluation of economic and energetic performance indicators (CAPEX, OPEX, COP, TAC).

This workflow converts process stream data into temperature–enthalpy profiles, defines feasible temperature intervals, and rapidly screens possible heat-pump allocations using ideal-performance estimates.

The output is a set of optimal temperature levels and associated heat duties that can later guide detailed superstructure design and optimization. The flowchart of this framework is illustrated in Figure 1.

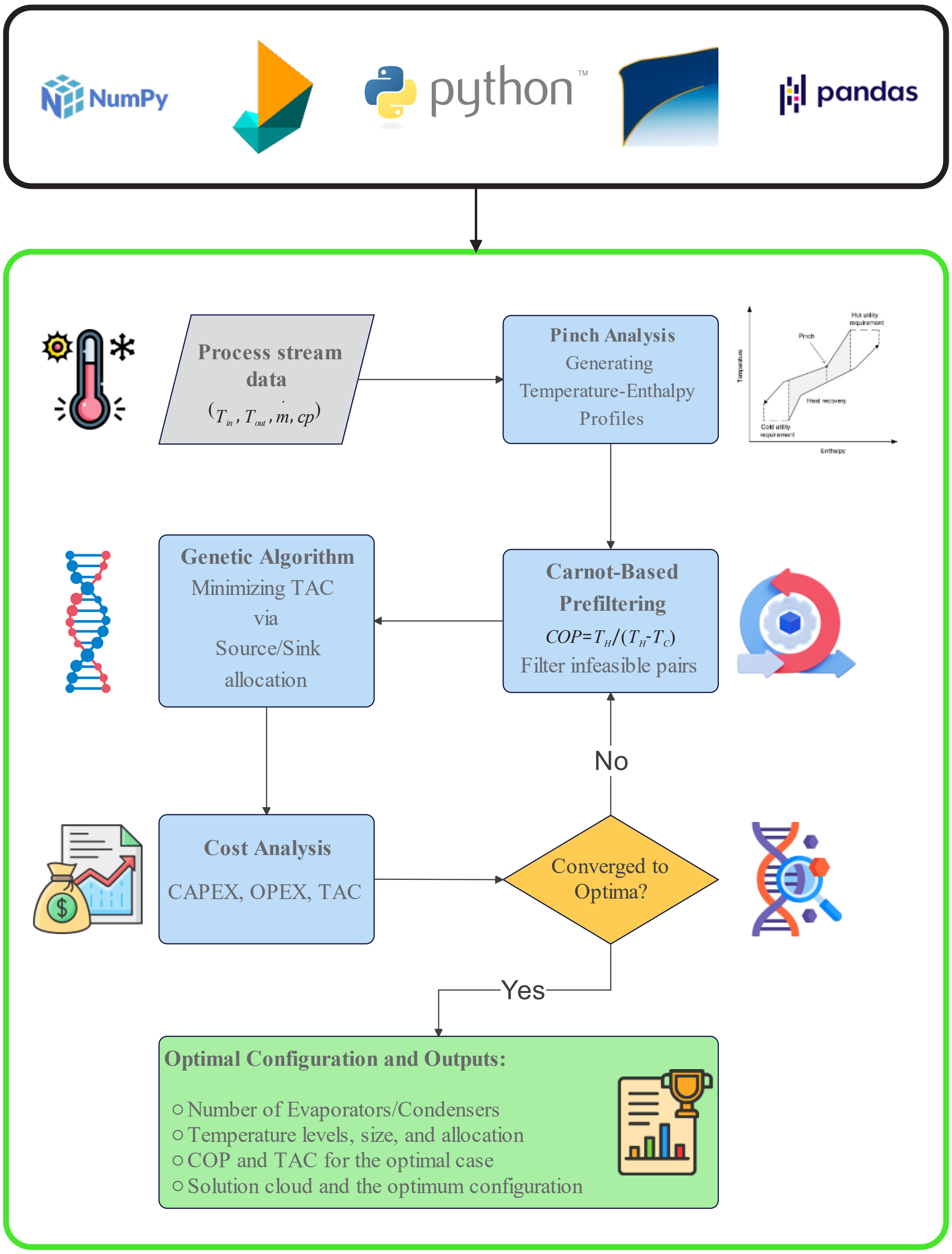

Figure 1. Workflow of the Carnot-based pre-screening and optimization procedure. Process data are analyzed through pinch analysis, evaluated thermodynamically using Carnot performance, and optimized using a Genetic Algorithm to minimize total annual cost.

2.2. Pinch-based representation of process data

Pinch analysis is used to extract the GCC of the process, representing cumulative heating and cooling requirements. After applying a minimum temperature approach (ΔT_{min}), the GCC is divided into source zones (heat available below the pinch) and sink zones (heat demand above the pinch). Each zone is characterized by different temperature levels and associated heat-flow potential ($\dot{Q}$).

$$\dot{Q}_i = \dot{m}_i \cdot c_{p,i} \cdot \left(\left|T_{i,out} - T_{i,in}\right|\right) \cdot 10^{-3} \tag{1}$$

Where $\dot{Q}_i$ denotes the heat duty of stream i in kW, $\dot{m}_i$ its mass flow rate in $kg \cdot s^{-1}$ and $c_{p,i}$ the specific heat capacity in $J \cdot (kg \cdot °C)^{-1}$.

The pinch temperature is determined when the temperature difference between hot and cold composite curves equals ΔT_{min}:

$$T_{pinch} = T_{cold,pinch} + \frac{\Delta T_{min}}{2} = T_{hot,pinch} - \frac{\Delta T_{min}}{2} \tag{2}$$

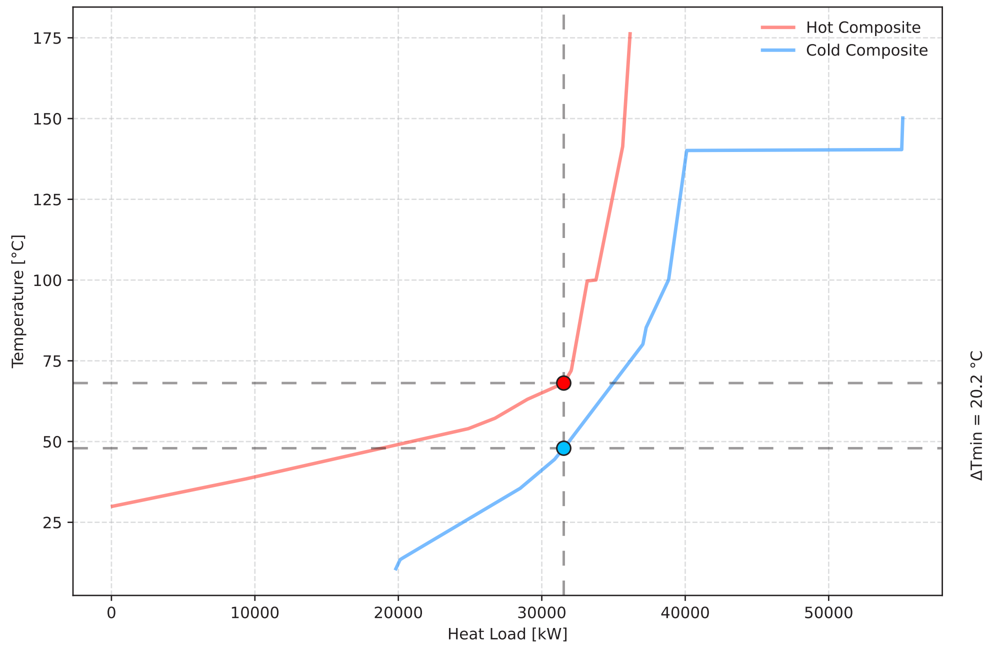

Figure 2. Composite Curves of the representative paper-mill process. The pinch point and minimum approach temperature (ΔT_{min}) define the thermodynamic boundary between available heat (red) and required heat (blue).

Figure 3 shows the GCC of a representative paper-mill process, where shaded regions highlight feasible temperature intervals for placing HTHP evaporators and condensers without violating the pinch constraint.

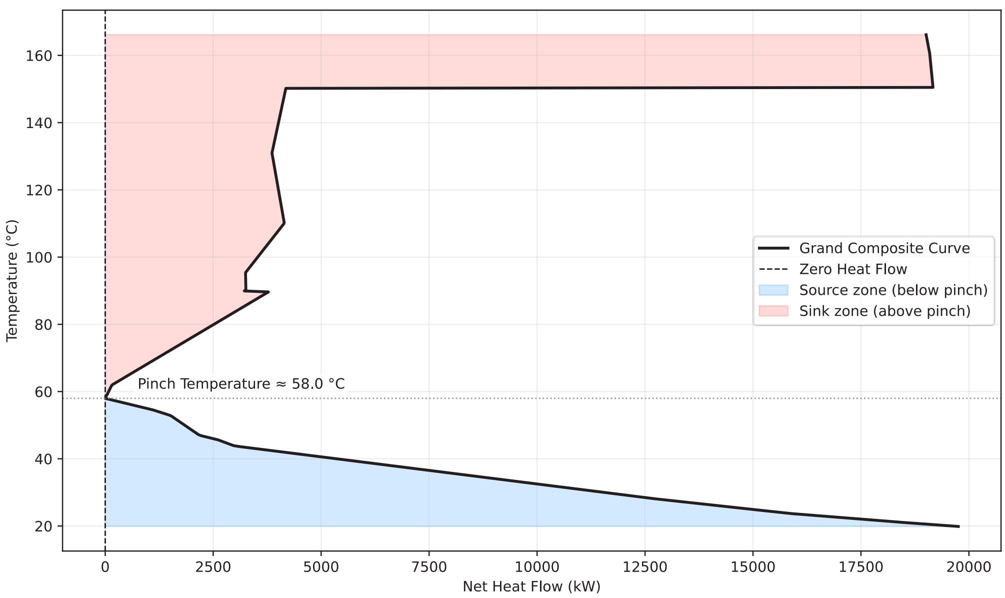

Figure 3. Source–sink zones from Pinch analysis indicating feasible regions for heat-pump integration.

2.3. Carnot-based thermodynamic screening

For each feasible source–sink pair, the theoretical efficiency of an ideal heat pump is calculated using the Carnot COP:

$$COP_{Carnot} = \frac{T_H}{T_H - T_C} \tag{3}$$

Where T_H and T_C in Kelvin (K) are the condenser and evaporator absolute temperatures.
The corresponding compressor work and extracted heat are:

$$W = \frac{Q_H}{COP_{Carnot}} \tag{4}$$

$$Q_C = Q_H - W \tag{5}$$

Although this idealized model neglects real-fluid irreversibilities, it preserves thermodynamic consistency and allows rapid comparison of thousands of potential configurations. High Carnot performance indicates strong potential for real-system integration, and it serves as a feasibility and ranking filter for subsequent optimization.

2.4. Optimization framework

The optimization problem aims to minimize the TAC while maintaining thermodynamic feasibility:

$$min\, TAC = \sum_i \left(CAPEX_{ann,i} + OPEX_{ann,i} \right) \tag{6}$$

Subject to:

$$T_H > T_C + \Delta T_{min}, \qquad COP_{Carnot} > 1 \tag{7}$$

Decision variables include the number of heat pumps, selected temperature levels, and corresponding heat duties. Because these involve both discrete (activation of temperature zones) and continuous (heat-flow) variables, the problem constitutes a MINLP formulation with multiple local optima. To avoid convergence to suboptimal solutions, a GA is employed.

Each individual in the GA population represents a configuration encoded as binary masks for activated source and sink zones. A stochastic allocation strategy evaluates each individual by randomly matching feasible source and sink zones to compute the overall COP and TAC. Selection, crossover, and mutation operators evolve the population toward lower-cost, higher-efficiency configurations until convergence.

2.5. Economic model and Performance metrics

Below, there are cost equations for TAC, and annualized capital and operational costs:

$$TAC = CAPEX_{ann} + OPEX_{ann} \tag{8}$$

$$CAPEX_{ann} = CAPEX \cdot CRF \tag{9}$$

$$CRF = \frac{r(1+r)^n}{(1+r)^n - 1} \tag{10}$$

$$OPEX_{ann} = C_{el} \cdot \dot{W} \cdot AOH + (0.02 \cdot CAPEX\,) \tag{11}$$

Here CRF is capital recovery factor, C_{el} is electricity price in USD/kWh, AOH is the annual operating hours, r the discount rate, $\dot{W}$ is the compressor's power consumption in kW, and n is the equipment lifetime which is assumed to be 20 years in this study. Also, it must be indicated that $CAPEX$ includes compressors, condensers, evaporators, and expansion valves, scaled according to heat-transfer area and compressor power. Table 1 presents some of the key design and optimization parameters.

Table 1. Key design and optimization parameters.

Category	Parameter	Value/Unit	Note
Economic Inputs	Electricity price	0.12 $USD \cdot kWh^{-1}$	Used in OPEX calculation
	Discount rate / Lifetime	5% / 20 years	For annualized CAPEX
	Maintenance cost	2% of CAPEX	Added to OPEX
Thermal Design	U-values (evap./cond.)	800 / 850 $W \cdot m^{-2} \cdot K^{-1}$	For HX sizing
	LMTD	Variable	Calculated based on location
Optimization setup	Population / Generations	500 / 70	GA configuration
	Crossover / Mutation	0.9 / 0.3	Probabilities
	Objective	Minimize TAC ($USD \cdot yr^{-1}$)	Includes CAPEX + OPEX

For every feasible configuration, two main indicators are evaluated:

- Overall COP, defined as total useful heat output divided by compressor work.
- Total annual cost, including annualized capital cost and operating cost (electricity and maintenance).

Because energy efficiency directly affects operating cost, the influence of COP is inherently reflected in the TAC. Together, these indicators provide a consistent thermodynamic and economic basis for comparing alternative temperature-level combinations and identifying the most promising candidates for detailed, real-fluid superstructure optimization.

3. Results and Discussion

3.1. Case study and optimization setup

The proposed optimization was applied to a representative paper-mill process characterized by heating and cooling demands between approximately 20 °C and 160 °C. Process data were discretized into temperature intervals derived from the Grand Composite Curve (GCC).

The Genetic Algorithm (GA) explored combinations of active source and sink zones using random source–sink allocation and evaluated each configuration through the Carnot-based thermodynamic model and cost function. Each population contained 500 individuals and evolved for 70 generations, leading to thousands of evaluated configurations covering a wide range of feasible heat-pump placements.

3.2. Convergence behavior

The GA explored a large, non-convex design space containing many thermodynamically feasible but economically distinct configurations. Figure 4 shows the evolution of the population across four representative generations. At the early stage, individuals are widely scattered over the COP–TAC domain, reflecting random initial exploration. As the optimization proceeds, the population gradually contracts into a well-defined Pareto-like region that reveals the trade-off between energy efficiency and cost.

In Figure 4, color represents the number of active evaporators, while symbol size indicates the number of source–sink allocations. Larger and brighter points generally correspond to configurations with higher complexity (more components) which can achieve higher COPs but also incur higher investment costs. By the final generation (bottom-right panel), the solutions cluster around a narrow band of near-optimal designs, showing that the GA effectively balances exploration and exploitation. This convergence behavior confirms the robustness of the stochastic search and highlights how Carnot-based screening allows thousands of configurations to be assessed rapidly while maintaining thermodynamic consistency.

All simulations were executed in Python using the DEAP evolutionary framework on a standard workstation (Intel i7, 16 GB RAM). The complete optimization run (70 generations $\times$ 500 individuals $\approx$ 35,000 evaluations) was completed in less than 1 minute, illustrating the computational efficiency of the Carnot-based pre-screening compared with traditional detailed thermodynamic optimization, which can require several hours/days for equivalent coverage of the design space.

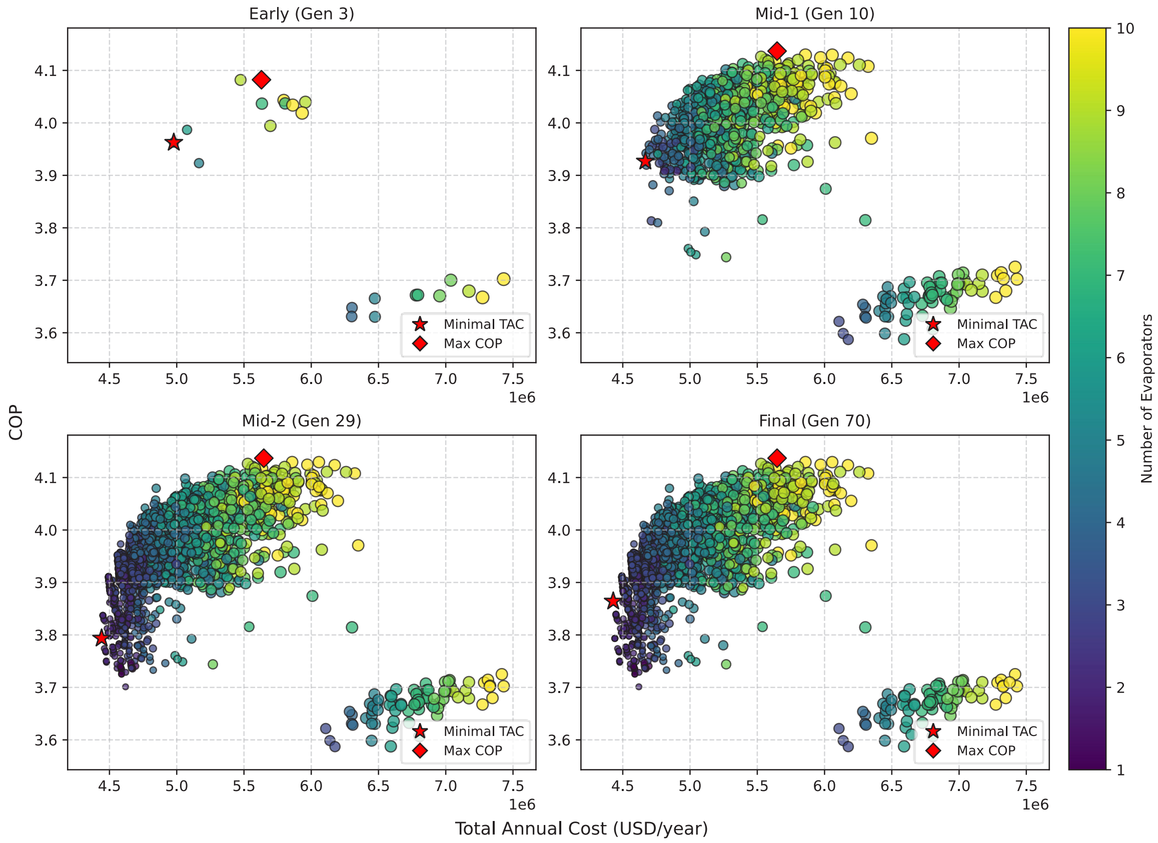

Figure 4. Evolution of the COP–TAC population across generations, showing convergence toward the optimal region and the trade-off between efficiency and cost (color = number of evaporators; size = number of allocations).

3.3. Optimal configuration

The best configuration found by the GA corresponds to one heat pump integrating two evaporators and two condensers, with three active allocations that determine how heat is exchanged between the selected temperature levels. This setup achieves an overall COP of 3.86 and a minimum TAC of 4.4×10^{6} USD/year. Table 2 summarizes the detailed heat flows and temperature levels of the selected matches.

Table 2. Best configuration obtained by the Genetic Algorithm.

T_{Source} (°C)	T_{Sink} (°C)	Q_C (kW)	Q_H (kW)	W (kW)	COP
36.7	150.5	7418.7	10143.9	2725.3	3.7
26.0	150.5	4016.8	5687.5	1670.7	3.4
26.0	85.0	2654.6	3178.2	523.5	6.0

Evaporators operated between 26 °C and 37 °C, extracting heat from waste streams below the pinch, while condensers supply heat at 85 °C and 150 °C, corresponding to medium and high-temperature process utilities. These allocations are overlaid on the process GCC in Fig. 3, demonstrating that all matches respect the pinch constraint and that the selected temperature intervals are thermodynamically feasible.

In Figure 5, these allocations are overlaid on the process GCC in Fig. 3, where green and red segments represent the extracted (Q_C) and supplied (Q_H) heat, respectively. All matches respect the pinch constraint, confirming the thermodynamic feasibility of the selected temperature intervals.

The optimized placement follows thermodynamic logic: extracting heat near the pinch reduces the required temperature lift, thereby increasing COP and lowering compressor work. The resulting configuration demonstrates that the Carnot-based pre-screening effectively guides the optimizer toward realistic and process-compatible solutions, balancing thermodynamic performance with economic efficiency. The distribution of feasible solutions in the final generation (Fig. 4, lower-right) also reinforces this result: configurations with additional components may offer marginally higher COPs but with sharply increasing TAC, emphasizing the existence of an optimal balance.

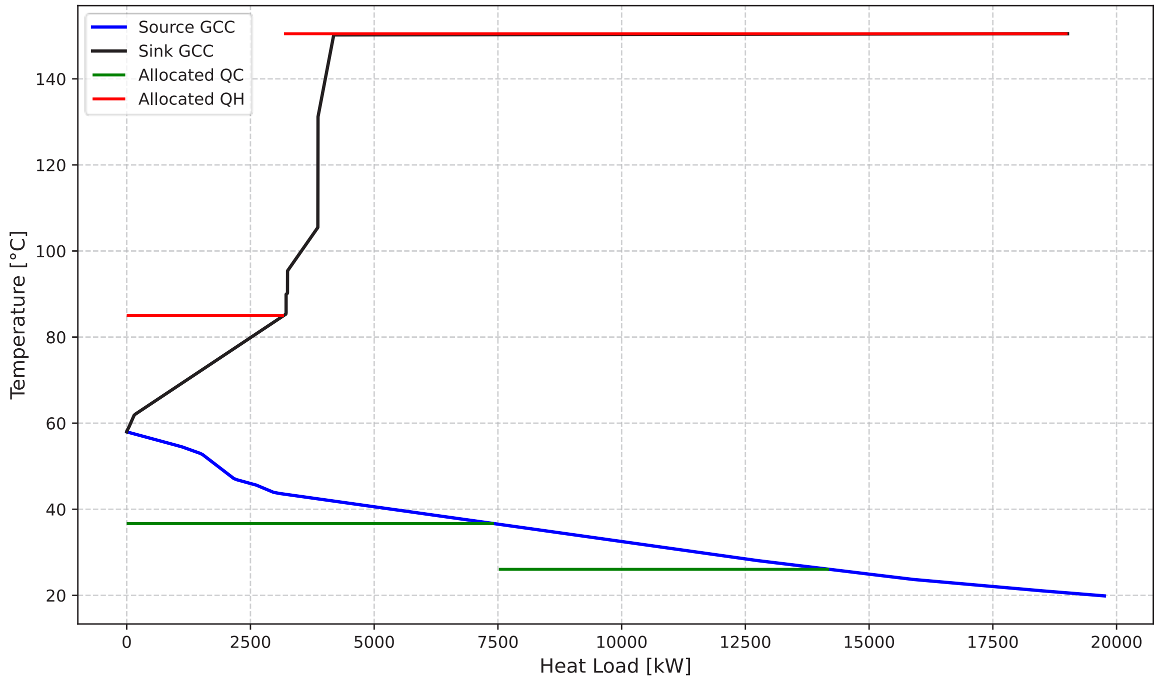

Figure 5. Optimal heat-pump allocations overlaid on the process GCC. Green = extracted heat (Q_C); red = supplied heat (Q_H).

3.4. Validation of Carnot-based pre-screening using a simplified real-cycle model

While the proposed framework relies on Carnot performance to rapidly screen and rank heat pump configurations, it is important to verify whether this ranking remains meaningful when evaluated with a more realistic thermodynamic model. To this end, the best solution identified by the Carnot-based GA at each generation was re-evaluated using a simplified single-stage vapor compression cycle with a fixed isentropic compressor efficiency. The same source–sink temperature levels and heat duties were preserved, enabling a direct comparison of COP and total annual cost (TAC) trends between the Carnot-based evaluation and a real-cycle approximation.

The real-cycle evaluation was carried out using a single-stage vapor compression cycle with water as the working fluid and a fixed isentropic compressor efficiency of 75%. For each source–sink match identified by the optimizer, an independent heat pump cycle was simulated, assuming 5 K of superheating at the compressor inlet, 3 K of subcooling at the condenser outlet, and isenthalpic expansion through the expansion valve. No explicit technical constraints on pressure ratio or discharge temperature were enforced, and all cycles were assumed to be operable in single-stage configuration. While simplified, this model captures the dominant thermodynamic and cost-driving mechanisms required for validation.

Figure 6 compares the evolution of COP and TAC across GA generations for both approaches. Although absolute values differ, both performance indicators exhibit very similar convergence behavior. Improvements identified by the Carnot-based optimization are consistently reflected in the real-cycle results, and the configuration identified as optimal by the Carnot-based GA also corresponds to the best-performing solution when evaluated with the real-cycle model. Minor oscillations observed in real-cycle TAC can be attributed to the nonlinear interaction between fixed compressor efficiency, component sizing, and cost scaling, but they do not affect the overall ranking or convergence of the optimal region.

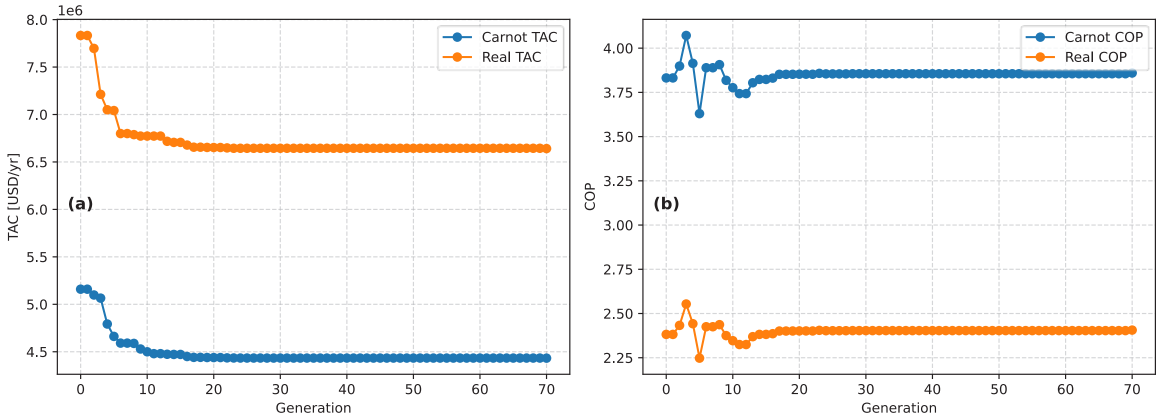

Figure 6. Evolution of (a) TAC and (b) COP over GA generations for Carnot-based and real-cycle evaluations.

This consistency is physically expected, as Carnot performance represents an optimistic upper bound on achievable efficiency. For a given source–sink temperature pair, the Carnot COP corresponds to the minimum theoretical compressor work and operating cost. Any real heat pump operating between the same temperature levels must therefore exhibit higher electricity consumption. Consequently, configurations that perform poorly even under Carnot assumptions are unlikely to become competitive when evaluated using more realistic cycle models. Conversely, configurations favored by Carnot-based screening correspond to placements with the highest thermodynamic potential, where real heat pumps can operate closest to the theoretical limit. The Carnot-based pre-screening thus identifies configurations with the largest margin for improvement, providing a robust and computationally efficient filter for subsequent detailed design.

Some deviations between Carnot-based and real-cycle results are expected due to simplifying assumptions adopted in the validation model, including fixed isentropic efficiency, the absence of pressure-ratio and discharge-temperature constraints, and the restriction to single-stage compression. These effects become more pronounced for large temperature lifts and dry working fluids, where multistage configurations or additional heat exchangers may be required. Despite these simplifications, the strong consistency observed in COP and TAC trends confirms the suitability of Carnot-based pre-screening as an initial design and ranking tool.

3.5. Sensitivity to ΔT_{min} and electricity price

To evaluate the robustness of the proposed framework under both process and economic uncertainties, a joint sensitivity analysis was conducted on the minimum temperature difference ΔT_{min} and the electricity price. Four ΔT_{min} values (0, 10, 20.2, and 30 K) and three electricity price levels (0.06, 0.12, and 0.24 USD/kWh) were considered. Figure 7 illustrates how ΔT_{min} modifies the GCC. Beyond shifting the pinch point toward lower temperatures, increasing ΔT_{min} also systematically increases both hot and cold utility demands: reducing the overlap between hot and cold composite curves limits internal heat recovery, so more external heating is required on the hot side while more low temperature heat must be rejected on the cold side. This structural effect is directly reflected in the GCC and translates into higher required heat pump duties and larger temperature lifts.

The corresponding optimal configurations are summarized in Table 3. The results confirm these thermodynamic trends at the system level: for all electricity price scenarios, increasing ΔT_{min} leads to a lower overall COP and a higher total annual cost (TAC). At low electricity prices, the optimizer tends to favor simpler configurations (fewer units) even if they involve larger temperature lifts, whereas higher electricity prices increasingly penalize inefficient heat pumping, leading to higher TAC and, in some cases, the activation of additional evaporator or condenser levels to mitigate efficiency losses. Despite these shifts, the optimizer consistently adapts the number and placement of heat pump units in a physically meaningful manner, demonstrating robustness under combined thermodynamic and economic uncertainty.

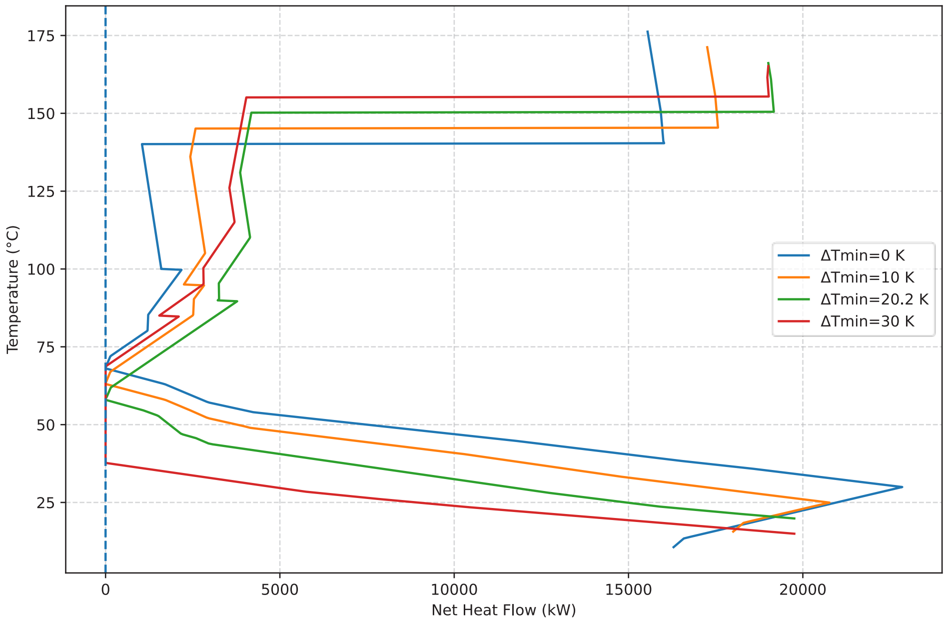

Figure 7. Effect of ΔT_{min} on the Grand Composite Curve (GCC) for the Papierfabrik Utzenstorf case.

Table 3. Sensitivity of optimal heat pump configuration to ΔT_{min} and electricity price (EP).

ΔT_{min} (K)	T_{Pinch} (°C)	EP (USD/kWh)	Evap.	Cond.	Alloc.	TAC (MUSD/yr)	COP
		0.06	1	2	2	1.85	4.46
0	68.1	0.12	1	2	2	3.10	4.47
		0.24	2	2	3	5.53	4.65
		0.06	1	2	2	2.19	4.09
10	63.1	0.12	2	2	3	3.71	4.27
		0.24	2	2	3	6.62	4.27
		0.06	1	2	2	2.60	3.67
20.2	58.0	0.12	2	2	3	4.43	3.86
		0.24	2	2	3	7.97	3.87
		0.06	1	2	2	2.87	3.22
30	37.8	0.12	1	3	3	4.93	3.35
		0.24	2	3	4	9.03	3.42

4. Conclusion

This work introduced a Carnot-based pre-screening methodology for the rapid and thermodynamically consistent integration of high-temperature heat pumps (HTHPs) into industrial processes.

By combining Pinch analysis, Carnot performance evaluation, and Genetic Algorithm (GA) optimization, the framework efficiently explores thousands of possible source–sink combinations and identifies cost-optimal configurations with minimal computational effort.

Applied to a representative paper-mill process, the approach revealed that configurations with additional components can reach slightly higher coefficient of performance (COP) but at significantly higher total annual cost (TAC), emphasizing the trade-off between energy efficiency and investment. The optimal solution identified two evaporators and two condensers operating between 26–37 °C and 85–150 °C, achieving an overall COP≈3.9 and a minimum TAC of about 4.4×10^6 USD/year.

A joint sensitivity analysis with respect to the minimum temperature difference (ΔT_{min}) and electricity price further demonstrated the robustness of the proposed framework. Increasing ΔT_{min} systematically reduced internal heat recovery, increased both hot and cold utility demands, and led to lower achievable COP and higher TAC across all economic scenarios. Higher electricity prices amplified these effects, while the optimizer consistently adapted the number and placement of heat pump units in a physically meaningful manner.

As expected, increasing condensation temperatures improves steam substitution potential, but the associated increase in temperature lift raises electricity demand, highlighting the importance of optimization to balance efficiency, cost, and decarbonization benefits. These results confirm that the Carnot-based pre-screening reliably identifies configurations with the highest thermodynamic potential under varying process and economic conditions.

The proposed Carnot-based pre-screening thus acts as a fast and scalable design filter, significantly narrowing the search space for subsequent real-fluid superstructure optimization. Beyond accelerating computational workflows, this method provides actionable insights for industrial decarbonization, enabling process engineers to quickly identify promising heat-pump integration options before detailed modeling.

Future developments will extend the framework to include real-fluid thermodynamics, compressor-efficiency correlations, and component-level cost models, allowing quantitative validation of the pre-screening results. The next step is the integration of these detailed models within a comprehensive superstructure, capable of representing multiple working fluids, cycle architectures, and process temperature levels in a single unified optimization environment. Such a superstructure is essential because the best design often depends on external factors such as energy prices, waste-heat availability, and process flexibility. By combining the speed of thermodynamic pre-screening with the rigor of detailed superstructure modeling, this approach can automatically identify cost-optimal and technically feasible, and low-carbon heat-pump solutions across a wide range of energy-intensive industries, supporting their transition away from fossil-fuel-based heating.

Acknowledgements

The author gratefully acknowledges the support and guidance of Prof. Martin Patel and the Energy Efficiency Group at the University of Geneva. This research was conducted as part of the doctoral work within the Institute for Environmental Sciences and received financial support from the Swiss Federal Office of Energy (SFOE) under the Industrial Decarbonization Program. The authors also thank the HPC 2026 Scientific Committee for providing the opportunity to present this work.

Nomenclature

Symbol	Description	Unit
AOH	Annual operating hours	hour
CAPEX	Capital expenditure	USD
$CAPEX_{ann}$	Annualized capital cost	USD · yr^{-1}
C_{el}	Electricity price	USD · kWh^{-1}
COP	Coefficient of performance (real)	–
COP_{Carnot}	Ideal Carnot coefficient of performance	–
c_p	Specific heat capacity	J · $(kg.°C)^{-1}$
ΔT_{min}	Minimum temperature approach	°C
LMTD	Log mean temperature difference	°C
n	Economic lifetime	years
$\dot{Q}$	Heat-transfer rate	kW
Q_H	Supplied heat (condenser duty)	kW
Q_C	Extracted heat (evaporator duty)	kW
r	Discount rate	–
T_H	Condenser temperature	K
T_C	Evaporator temperature	K
T_{pinch}	Pinch temperature	°C
TAC	Total annual cost	USD · yr^{-1}
U	Overall heat-transfer coefficient	W · m^{-2} · K^{-1}
$\dot{W}$	Compressor power input	kW
ΔT	Temperature difference (lift)	°C
GA	Genetic Algorithm	–
GCC	Grand Composite Curve	–
HTHP	High-Temperature Heat Pump	–
MINLP	Mixed-Integer Nonlinear Programming	–
OPEX	Operational expenditure	USD · yr^{-1}

References

[1] IEA. CO2 Emissions in 2022 – Analysis - IEA. Global Energy 2023;62.

[2] Kong L, Hasanbeigi A, Price L. Assessment of emerging energy-efficiency technologies for the pulp and paper industry: a technical review. J Clean Prod 2016;122:5–28. https://doi.org/10.1016/j.jclepro.2015.12.116.

[3] Sadeghi M, Petersen T, Yang Z, Zühlsdorf B, Madsen KS. Thermal and economic performance assessment of different high temperature heat pump layouts for upgrading district heating to process heating of steam production at 160°C. Energy 2024;313:133832. https://doi.org/10.1016/j.energy.2024.133832.

[4] Babaei SM, Patel MK. Optimizing energy use in the pulp and paper industry: Pinch, techno-economic, and sensitivity analyses on an innovative heat recovery system. J Clean Prod 2025;520:146109. https://doi.org/10.1016/j.jclepro.2025.146109.

[5] Mostafa Babaei S, Patel MK. Deep decarbonization of the pulp and paper industry: Heat integration and techno-economic analysis combined with tailored heat pumps. Energy 2025;338:138881. https://doi.org/10.1016/J.ENERGY.2025.138881.

[6] Schlosser F, Arpagaus C, Walmsley TG. Heat pump integration by pinch analysis for industrial applications: A review. Chem Eng Trans 2019;76:7–12. https://doi.org/10.3303/CET1976002.

[7] Wallerand AS, Kermani M, Kantor I, Maréchal F. Optimal heat pump integration in industrial processes. Appl Energy 2018;219:68–92. https://doi.org/10.1016/J.APENERGY.2018.02.114.

[8] Sharevska M, Sharevska M, Brem G, Hoogsteen G, Hurink J, Hajimolana Y. Systematic integration of high temperature heat pumps in industrial multi-energy systems. Appl Therm Eng 2025;278:127440. https://doi.org/10.1016/J.APPLTHERMALENG.2025.127440.

[9] Walden JVM, Padullés R. An analytical solution to optimal heat pump integration 2024. https://doi.org/10.1016/j.enconman.2024.118983.